

## EXPERIMENTAL STUDY OF A PULSATING HEAT PIPE USING FC-72, ETHANOL, AND WATER AS WORKING FLUIDS

X. M. Zhang, J. L. Xu, and Z. Q. Zhou

Guangzhou Institute of Energy Conversion, Chinese Academy of Sciences,  
Guangzhou, People's Republic of China

*Experimental studies were performed on a pulsating heat pipe (PHP), consisting of a heating section, an adiabatic section, and a condensation section incorporating a heat sink. The capillary tube used in this study has an inside diameter of 1.18 mm and a wall thickness of 0.41 mm. The experiments were conducted under the condition of pure natural convection, for heating powers from 5 to 60 W, fill ratios from 60% to 90%. Three working fluids—FC-72, ethanol, and deionized water—were used. The thermal oscillation of the thin wall surface was recorded by a high-speed data acquisition system. Such thermal oscillation waves are random for some run cases due to the randomly distributed vapor plug and liquid slugs inside the PHP. The thermal oscillation amplitude is much smaller for FC-72, due to its lower surface tension, than for ethanol and water, while the oscillation cycle period for FC-72 is shorter than for the other two fluids, indicating the faster oscillation movement in the channels, possibly due to the lower latent heat of evaporation for FC-72. The unlooped PHP is not helpful for the fluid circulation and the PHP does not work. For the looped PHP, there is a minimum heating power that initiates the PHP working. Such minimum heating power is strongly dependent on the working fluid, and is considerably smaller for FC-72 compared with water. The optimal filling ratio is around 70% for all three working fluids. The looped PHP with water as working fluid provides better overall thermal performance once the heating power is greater than a minimum value. However, FC-72 is suggested to be used for low-heat-flux situations, due to its lower minimum heating power.*

In recent years, due to the fast development of integrated circuit chips and semi-conductors, novel electronic cooling devices have to be developed. The pulsating heat pipe (PHP), which was first proposed by Akachi [1] in 1990, is a possible solution for the electronic thermal management system. Since the introduction of the PHP, some experimental and analytical/numerical work has been conducted. The dynamic vapor/liquid slugs were visualized to be moving up and down periodically inside the glass capillary tube qualitatively [2–4].

Wong et al. [5] proposed a theoretical model in terms of a Lagrangian approach in which the flow was modeled at adiabatic conditions for the whole PHP. A sudden pressure pulse was applied to simulate the heat input over a vapor plug. They could show the

Received 18 May 2003; accepted 8 August 2003.

Address correspondence to Dr. J. L. Xu, Guangzhou Institute of Energy Conversion, Chinese Academy of Sciences, No. 81 Xianlie Zhong Rd., Guangzhou, 510070, People's Republic of China. E-mail: xujl@ms.giec.ac.cn

### NOMENCLATURE

<p><math>C_p</math> specific heat, J/kg K</p> <p><math>d</math> inside tube diameter, m or mm</p> <p><math>g</math> gravity acceleration, <math>m/s^2</math></p> <p><math>H_{fg}</math> latent heat of evaporation, J/kg</p> <p><math>k</math> thermal conductivity, W/m K</p> <p><math>M</math> full cycles in a given integrated time</p> <p><math>N</math> total number of data points in a given integrated time</p> <p><math>P</math> pressure, Pa</p> <p><math>q</math> heat flux, <math>W/m^2</math></p> <p><math>r</math> radius, m</p> <p><math>T</math> temperature, <math>^{\circ}C</math></p> <p><math>\alpha</math> heat transfer coefficient, <math>W/m^2 K</math></p> <p><math>\Delta T_{\text{mean, amplitude}}</math> mean temperature oscillation amplitude versus the mean value</p>	<p><math>\rho</math> density, <math>kg/m^3</math></p> <p><math>\sigma</math> surface tension, N/m</p> <p><b>Subscripts</b></p> <p>cold cold cold side (condensation section)</p> <p><math>f</math> liquid state</p> <p>film film thin liquid film</p> <p><math>g</math> vapor state</p> <p>hot hot hot side (heating section)</p> <p>in inner wall surface</p> <p>mean mean mean value</p> <p>out out outer wall surface</p> <p>peak peak peak value in a given cycle</p> <p>sat sat saturation</p> <p><math>w</math> wall</p>
---	--

pressure and velocity variations versus time for the vapor plugs. Dobson and Harms [6] proposed simple mathematical models in which the behavior of the unlooped PHP was simulated. They concluded that the calculation results relied on the different initial given values. Very recently, Shafii et al. [7, 8] performed a numerical simulation of both unlooped and looped PHPs with multiple liquid and vapor plugs using the constant wall temperature condition. They illustrated that the gravity force has an insignificant effect on the performance of the PHP. They also demonstrated that the major heat transfer mechanism is due to the sensible heat and the PHP does not work at high fill ratios such as higher than 90%.

In the present study, we present detailed thermal oscillation measurements of the thin wall surface of a PHP. Three working fluids—FC-72, ethanol, and deionized (DI) water—are used. The present report contains important experimental findings on thermal oscillations, comparisons between looped and unlooped PHP, minimum heating power initiating the device working, optimal fill ratio, etc. Such findings are useful both for the practical design and operation of PHPs, and for understanding the PHP thermal-fluidic transport phenomena inside the capillary tube.

### THE PHP AND ITS WORKING PRINCIPLE

If the inside diameter of a capillary tube is small enough, such as  $d \leq 1.83\sqrt{\sigma/g(\rho_f - \rho_g)}$ , evacuating the tube and then partially charging the tube with liquid can form randomly distributed liquid slug and vapor plugs. Bending the long capillary tube into many turns periodically can form a snake-shaped PHP. There are many types of PHP designs in the Akachi patent [1]. However, these designs can be subdivided into two categories: looped and unlooped PHPs. The structures are characterized by the following features.

The PHP can work without an internal wick structure, leading to very low fabrication cost.

However, a PHP with a wick structure can greatly enhance the heat transfer [9].

Generally there are heating, adiabatic, and condensation sections. The heating section receives heat and the condensation section rejects the heat to the heat sink or the environment. The adiabatic section separates the heating and condensation sections. The PHP is a passive device that works by self thermally driven oscillation, without any mechanical moving parts.

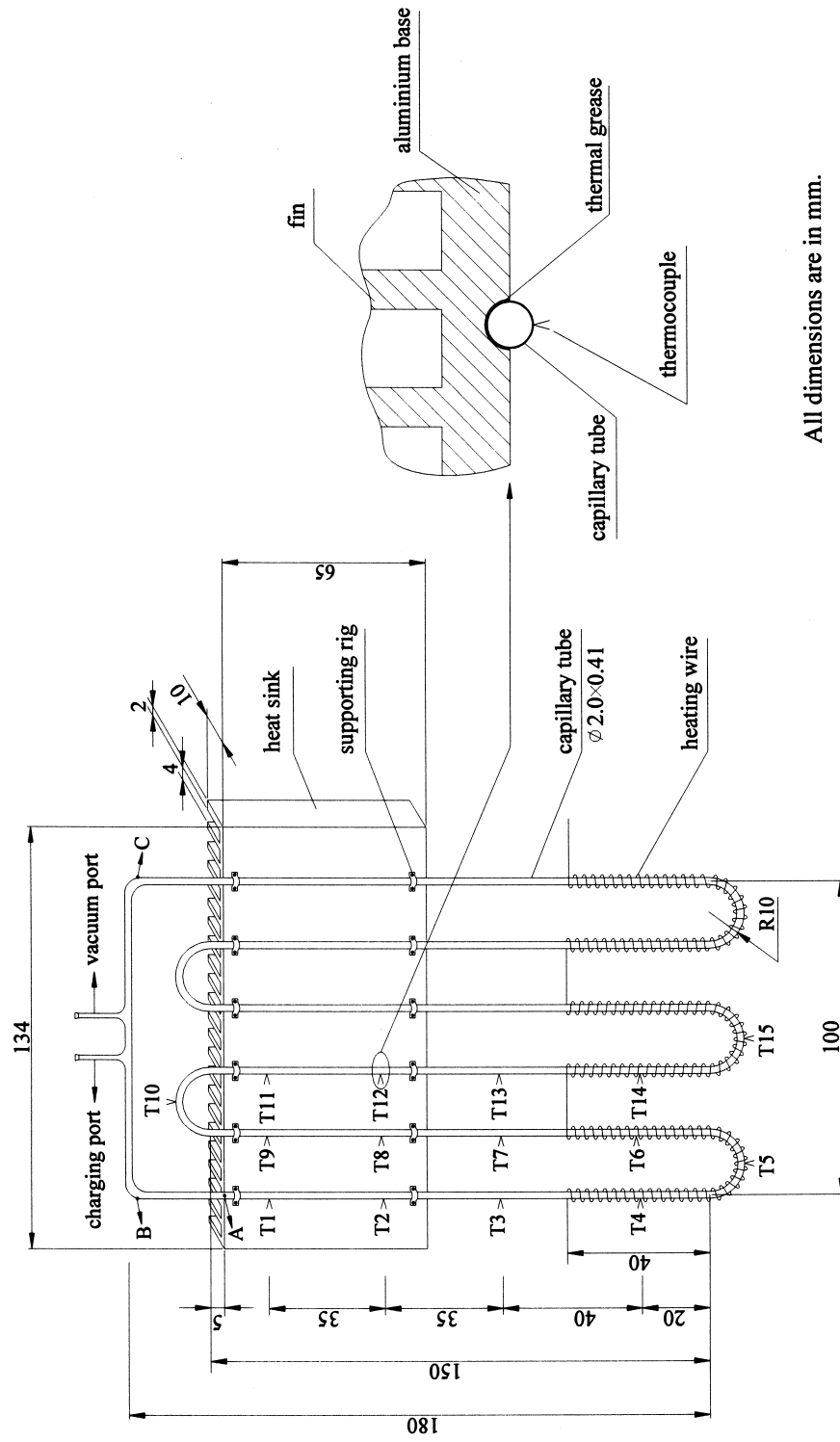
Both the latent and sensible heat may serve as the heat transfer mechanism. The numerical modeling by Shafiq et al. [7, 8] indicates that the major heat is transferred by the sensible heat, not the latent heat.

The surface tension dominates the flow and heat transfer inside the capillary tube.

In an actual working PHP, there are pressure and temperature gradients between the heating and condensation sections. In addition to these, heat received from the heating section leads to uneven pressure distributions among the parallel channels due to the uneven vapor expansion in the parallel channels resulting from the unevenly distributed vapor plugs in the parallel channels. Such pressure differences between the heating and condensation sections, and among the parallel channels, result in fluid transport among the parallel channels. Therefore self-sustained thermally driven oscillating flow is maintained in a PHP. Once thermally driven oscillating flow is initiated inside the whole PHP, heat is transferred from the heating section to the condensation section by the oscillating two-phase convection. Boiling takes place in the heating section, while condensation occurs in the condensation section. The working process of the PHP is a dynamic one, quite distinct from that of the conventional micro-heat pipes using wick structures.

## EXPERIMENTAL SETUP

Figure 1 illustrates the PHP used in the present study, with an overall width of 100 mm and a height of 180 mm. The PHP was fabricated using a long copper capillary tube with an outside diameter of 2.0 mm and an inside diameter of 1.18 mm. The bending radius is 10 mm. Heating, adiabatic, and condensation sections are included in the PHP. In the heating section, the thermal load was applied by Ni-Cr thermic wire with a diameter of 0.4 mm ( $12 \Omega/\text{m}$ ) which was wrapped at intervals of 1.5 mm on the outer wall surface of the heating section. The heat sink is made of aluminum with dimensions  $134 \times 65 \times 10 \text{ mm}^3$  with a fin height of 8.0 mm, a thickness of 2.0 mm, and a gap distance of 4.0 mm. Below the heat sink the capillary tube is well heat-insulated by the thick heat insulation material, forming the adiabatic and the heating sections. The present PHP is a closed-loop one, with one vacuum port and another charging port. The alternative design is the unlooped PHP, with the capillary tube ending at points B and C serving as the charging and vacuum ports. In all, 15 fine K-type thermocouple wires of diameter of 0.1 mm are attached on the outer wall surface of the capillary tube by soldering. These thermocouples cover exactly half of the whole PHP, which is necessary to give information about the whole PHP due to the configuration symmetry at T15. The thermocouples are numbered from T1 to T15; among them, T4, T5, T6, T14, and T15 are located in the heating section, T3, T7, and T13 are at the wall surface of the adiabatic section, while T1, T2, T8, T9, T11, and T12 are located in the condensation (heat sink) section. The capillary tube is well embedded in the heat sink by filling with thermal grease in between, as also shown in Figure 1. Assuming the capillary tube was straightened starting from point A, each thermocouple has a corresponding axial distance



All dimensions are in mm.

Figure 1. Test section of the present PHP.

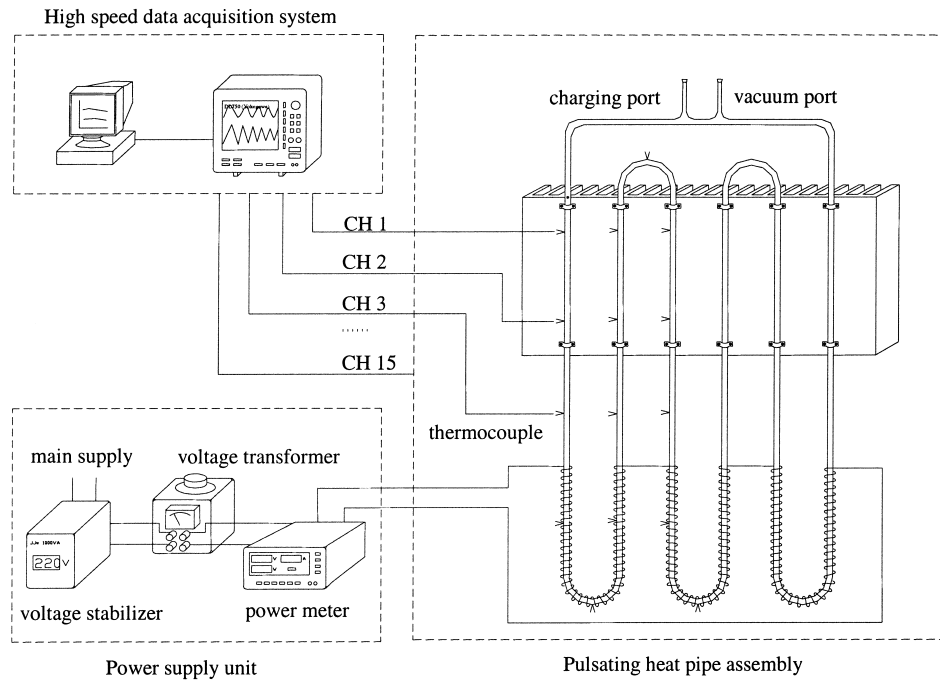
**Table 1.** Corresponding axial thermocouple locations (mm)

T1	T2	T3	T4	T5	T6	T7	T8	T9	T10	T11	T12	T13	T14	T15
15	50	85	125	161	196	236	271	306	342	378	413	448	488	524

from T1 (15 mm) to T15 (524 mm), as shown in Table 1, while T15 is located at the centerline of the whole PHP.

The experimental setup, as shown in Figure 2, consists of the power supply unit, the PHP unit, and the high-speed data acquisition system. The power supply unit includes an AC voltage stabilizer, a voltage transformer, and a power meter. By adjusting the voltage transformer, one can obtain a stable voltage output in the range of 2–220 V, resulting in controlled adjustable heating power in the range from 1 to 500 W. The power meter measures the voltage, current, and heating power simultaneously supplied on the heating section. The present heating setup forms the constant heat flux boundary condition for the heating section.

A high-speed data acquisition system (DL750, Yokogawa, Inc., Japan) with 16 channels was used in the present study. The data sampling rate can be up to 100 K samples per second. For the present applications, we use the data acquisition system to measure the thermal oscillation at the capillary tube wall surface using a sampling rate of 500/s. Assuming the capillary tube, with a total length of 1.0 m, was bent to form six parallel channels and there are 10 vapor plugs and liquid slugs in each channel, the

**Figure 2.** Experimental setup.

**Table 2.** Saturated thermophysical properties of different liquid coolants at 1 atm

Fluid	$T_{\text{sat}}$ (°C)	$\rho_f$ (kg/m <sup>3</sup> )	$\rho_g$ (kg/m <sup>3</sup> )	$C_{P,f}$ (J/kg °C)	$H_{fg}$ (kJ/kg)	$\sigma$ (N/m)
FC-72	56.6	1,600	13.43	1,102	94.8	$8.35 \times 10^{-3}$
Ethanol	78.3	757	1.57	2,580	960.0	$17.46 \times 10^{-3}$
Water	100	958	0.60	4,217	2,256.7	$58.91 \times 10^{-3}$

length of each vapor plug/liquid slug is 16.0 mm. Again the flow velocity of the mixtures is of the order of 1.0 m/s, thus the time during which the vapor plug/liquid slug passes through a specific wall surface is around 16.0 ms. The data sampling rate of 500/s is fast enough to capture the dynamic process with a time scale of 16 ms. The thermocouples are carefully calibrated using a constant-temperature bath with an accuracy of 0.1°C. The power supply has an error of less than 1%.

The vacuum and charging procedures are performed using a special facility fabricated in our laboratory. The PHP is baked at 150°C, evacuated to a pressure of  $7.5 \times 10^{-4}$  torr for 8 h, and then isolated from the vacuum system by seal. The PHP is then filled with the working fluid, and sealed. In order to study the effect of physical properties on the thermal performance of the PHP, three working fluids, FC-72, ethanol, and DI water, were used in the present study. The final net liquid charged inside the PHP is the weight difference before and after the PHP was charged with liquid. Such weight measurements are performed by an electronic balance with the accuracy of 0.01 g. The total inside volume of the PHP is 1.32 ml. The fill ratio is defined as the liquid volume occupied by the total inside volume of the PHP. The fill ratio is estimated to have an uncertainty of 1%.

The PHP assembly is arranged in the vertical plane. Heat is received in the heating section, transferred to the condensation section, and finally dissipated to the environment by the pure natural-convection heat transfer between the heat sink and the air. The room temperature is well kept at 24°C with an uncertainty of 1°C. In the test procedure, the thermal oscillation is monitored on the screen of the data acquisition system. The data is transferred to a personnel computer after a steady oscillation state is reached.

The important physical properties for the three working fluids are listed in Table 2. The present inside tube diameter of 1.18 mm satisfies the tube diameter criteria of  $d \leq 1.83\sqrt{\sigma/g(\rho_f - \rho_g)}$  for all three working fluids.

## ANALYSIS OF THE THERMAL OSCILLATION

It is difficult to measure the fluid temperatures inside the small-size capillary tube. The present study is to measure the dynamic temperatures at the outer wall surface, and try to connect the wall thermal oscillation with the fluid transport phenomena inside the tube. First we estimate the temperature difference between the outer and the inner wall surfaces. The measured outer wall temperatures can be converted to the inner wall temperatures, using the one-dimensional steady-state heat conduction equation, assuming constant copper thermal conductivity:

$$T_{w,\text{in}} = T_{w,\text{out}} - \frac{q_{w,\text{out}} r_{\text{out}}}{k} \ln \frac{r_{\text{out}}}{r_{\text{in}}} \quad (1)$$

For the maximum heating power of 60 W, the corresponding heat flux in terms of the outer wall surface is 28.58 kW/m<sup>2</sup>, the temperature difference between the outer and the inner wall surface is 0.04°C, using the copper thermal conductivity of 393 W/m°C at 100°C. For the heating power of 20 W, the temperature difference is only 0.01°C. The temperature difference between the inner and the outer wall surfaces is one order less than the fine thermocouple accuracy. Also, due to the thin tube wall and the high copper thermal conductivity, the outer wall surface has a very short response time following the temperature changes of the inner wall surface. Therefore the outer wall surface thermal oscillation can represent the temperature variation of the inner wall surface which is contacted with the dynamic vapor plug/liquid slug flow.

Now we turn to analyzing the thermal oscillation of the wall surface resulting from the dynamic vapor plug/liquid slug flow. Four conditions are considered.:

1. *In the heating section, the local wall surface is temporarily immersed in the vapor plug region, as shown in Figure 3a.*

Vapor plugs and liquid slugs coexist in the capillary tubes, as shown in Figure 3. In the vapor plug region, there is a thin liquid film separating the vapor plug body and the tube wall surface. The thin liquid film provides a higher-boiling heat transfer coefficient. Evaporating takes place at the vapor/liquid interface. Across the vapor/liquid interface, the pressure difference between the vapor side and the liquid side is written as

$$P_g - P_f = \frac{2\sigma}{r} \quad (2)$$

where  $r$  is the meniscus radius of the vapor/liquid interface. The vapor plug temperature  $T_g$  should be at least the saturated temperature corresponding to the pressure  $P_g$ . That is,  $T_g \geq T_{\text{sat}}(P_g)$ . Because the evaporating heat and mass transfer is taking place at the vapor/liquid interface, the liquid temperature  $T_f$  should be larger than  $T_g$ , that is,

$$T_f > T_g \geq T_{\text{sat}}(P_g) \quad (3)$$

The local wall surface temperature is

$$T_{w,\text{in}} = T_g + \frac{q_{w,\text{in}}}{\alpha_{\text{film}}} \quad (4)$$

where  $\alpha_{\text{film}}$  is the heat transfer coefficient due to the thin film evaporation.

2. *In the heating section, the local wall surface is temporarily immersed in the liquid slug region, as shown in Figure 3b.*

The analysis of the vapor plug/liquid slug is described above. The local wall surface temperature is

$$T_{w,\text{in}} = T_f + \frac{q_{w,\text{in}}}{\alpha_{\text{liquid}}} \quad (5)$$

where  $\alpha_{\text{liquid}}$  is the liquid forced-convection heat transfer coefficient, which is smaller than  $\alpha_{\text{film}}$ . Because  $T_f > T_g$  and  $\alpha_{\text{liquid}} < \alpha_{\text{film}}$ , the wall surface temperature when the

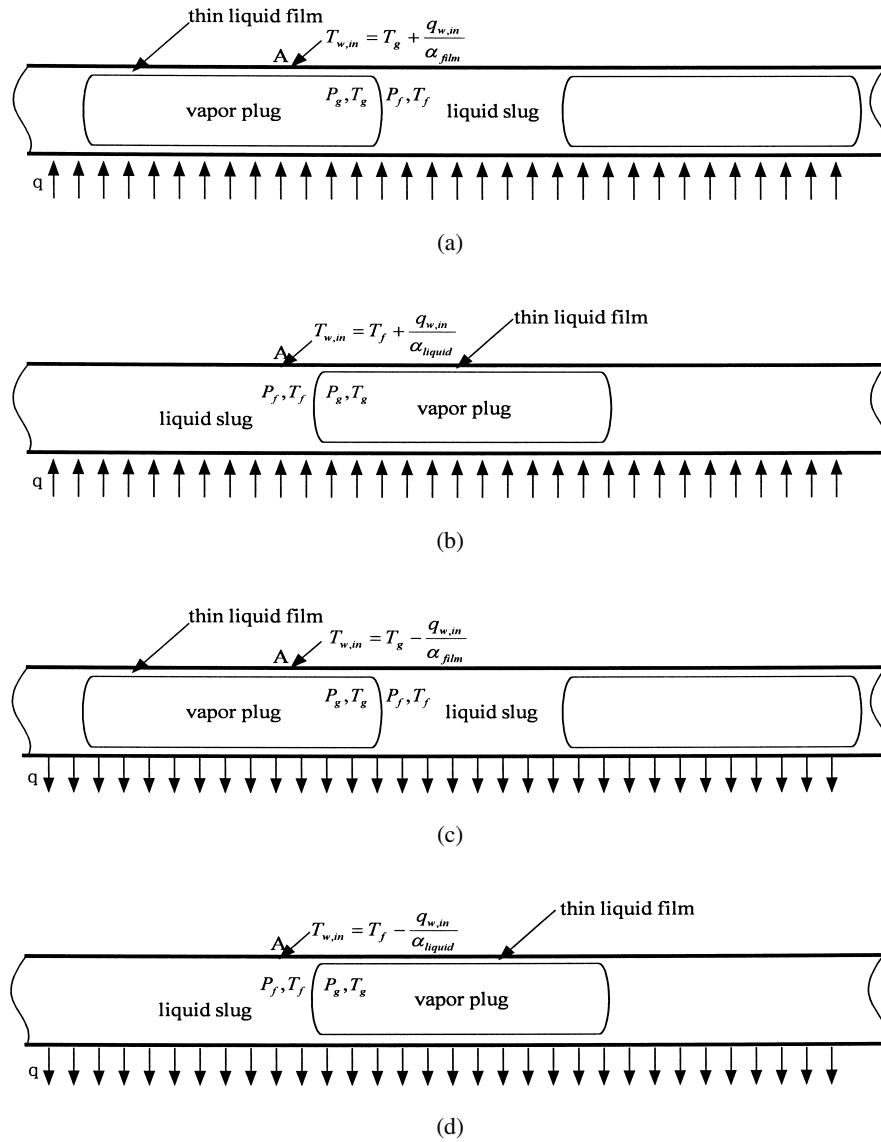


**Figure 3.** (a) Local wall surface is immersed in the vapor plug region, heating section. (b) Local wall surface is immersed in the liquid slug region, heating section. (c) Local wall surface is immersed in the vapor plug region, condensation section. (d) Local wall surface is immersed in the liquid slug region, condensation section.

local point is located in the liquid slug region in terms of Eq. (5) should be larger than that when the local wall surface is immersed in the vapor plug region by Eq. (4).

For the pulsating heat pipe, any local wall surface is flushed alternatively by the vapor plug and the liquid slug. When the local wall surface begins to be flushed by the liquid slug, the local temperature shows a sharp increase. When the local surface is flushed by the vapor plug, the local temperature shows a sharp decrease. This process repeats continuously, forming the thermal oscillation of the wall surface.



In the condensation section, an inverse process takes place, as shown in Figures 3c and 3d. Because the condensation heat transfer occurs at the vapor/liquid interface, the vapor plug should have higher temperatures than the liquid slug. Therefore the wall surface has higher temperatures when it is immersed in the vapor plug region, while it has lower values when the wall surface is flushed by the liquid slug. The oscillation movement results from the local surface periodically immersed in the vapor plug and liquid slug regions. The process repeats and thermal oscillation occurs.

## RESULTS AND DISCUSSION

### Measurement of the Thermal Oscillation

Because the randomly distributed vapor plug and liquid slugs inside the capillary tube, the thermal oscillation wave should not be very standard. Thus a simple technique is used to decide the mean oscillation parameters, such as mean temperature, mean cycle period, and mean oscillation amplitude. The mean temperature is defined as the sum of the transient temperatures over a given integrated time, which is much longer than a full cycle period:

$$T_{\text{mean}} = \frac{\sum_{i=1}^N T_i}{N} \quad (6)$$

where  $N$  is the total number of data points including in the given time period, such as 100 s. The mean oscillation cycle period is defined as the integrated time divided by the total number of full cycles. The mean oscillation amplitude is the averaged oscillation amplitude over the given integrated time, which is written as

$$\Delta T_{\text{mean, amplitude}} = \frac{\sum_{j=1}^M T_{j, \text{peak}} - T_{\text{mean}}}{M} \quad (7)$$

where  $T_{j, \text{peak}}$  is the peak temperature value for cycle  $j$ . There are  $M$  full cycles in the given integrated time. Once the PHP is working at the steady oscillation state, the above mean statistical values should be insensitive to the given integrated time, whether 100 or 200 s.

Typical thermal oscillation profiles for the looped PHP with FC-72 as working fluid, fill ratio of 0.702, and heating power of 50.2 W are illustrated in Figure 4. T5 (heating section) is detected to be always oscillating against a mean value periodically. The mean temperature is 141.13°C, while the mean cycle period is 0.56 s (36 full cycles included in 20 s). The difference between minimum and maximum temperature is found to be around 1°C. The mean oscillation amplitude was computed as 0.36°C. The thermal oscillation measurements confirm the above analysis qualitatively, indicating the nonequilibrium temperature across the vapor/liquid interface.

The thermal oscillations for the adiabatic (T3) and condensation (T2) sections cannot follow the same thermal oscillation cycles as the heating section. Such oscillations are quite small, indicating smaller nonequilibrium temperature across the vapor/liquid interfaces, compared with the heating section.

Typical thermal oscillations for the looped PHP with ethanol, fill ratio of 0.818, and heating power of 49.8 W, are shown in Figure 5. It is found that the thermal oscillations

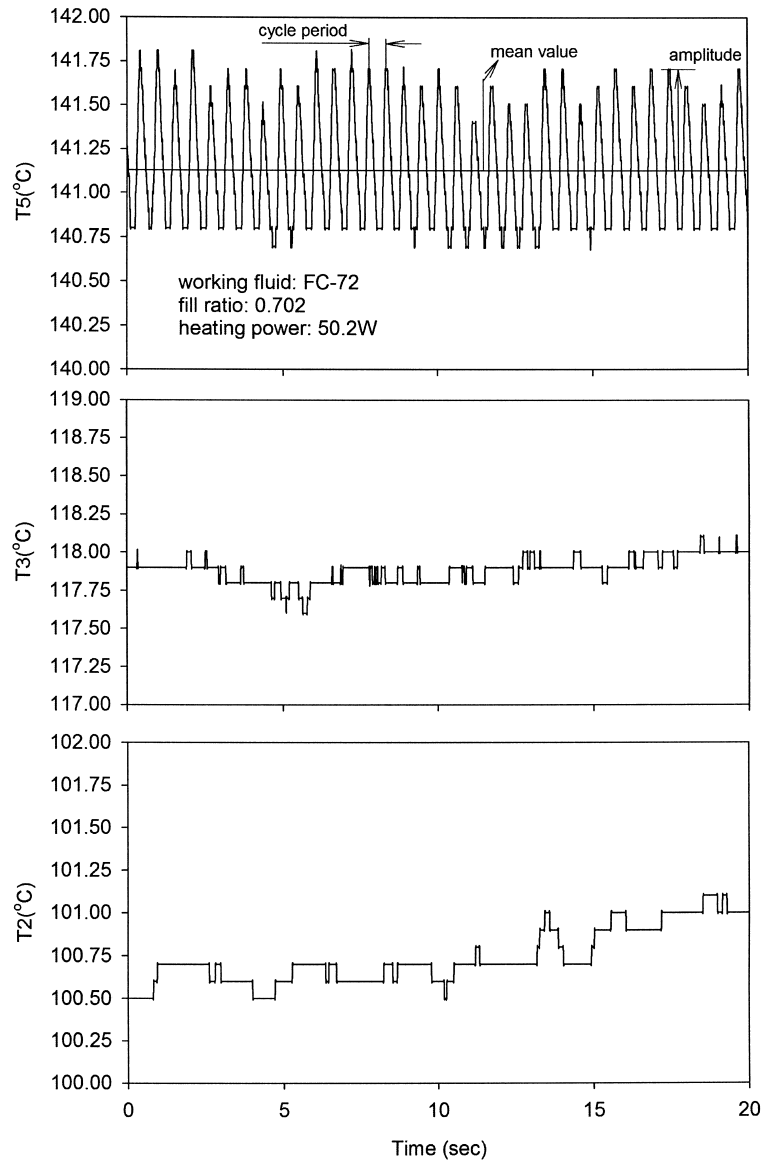


**Figure 4.** Thermal oscillation of the wall surface for FC-72.

in the heating (T5), adiabatic (T3), and condensation (T8) sections share the same cycle period. The cycle period is estimated to be 2.63 s (19 full cycles cover the time of 50 s). The mean values of T5, T3, and T8 are 128.6, 95.1, and 98.6°C, respectively. The mean oscillation amplitudes are 1.15, 1.45, and 0.98°C, respectively.

The thermal oscillations were also detected with water as working fluid, as shown in Figure 6. However, the thermal oscillation waves are much more random, thus a special thermal oscillation wave analysis should be further provided. From Figure 6 we

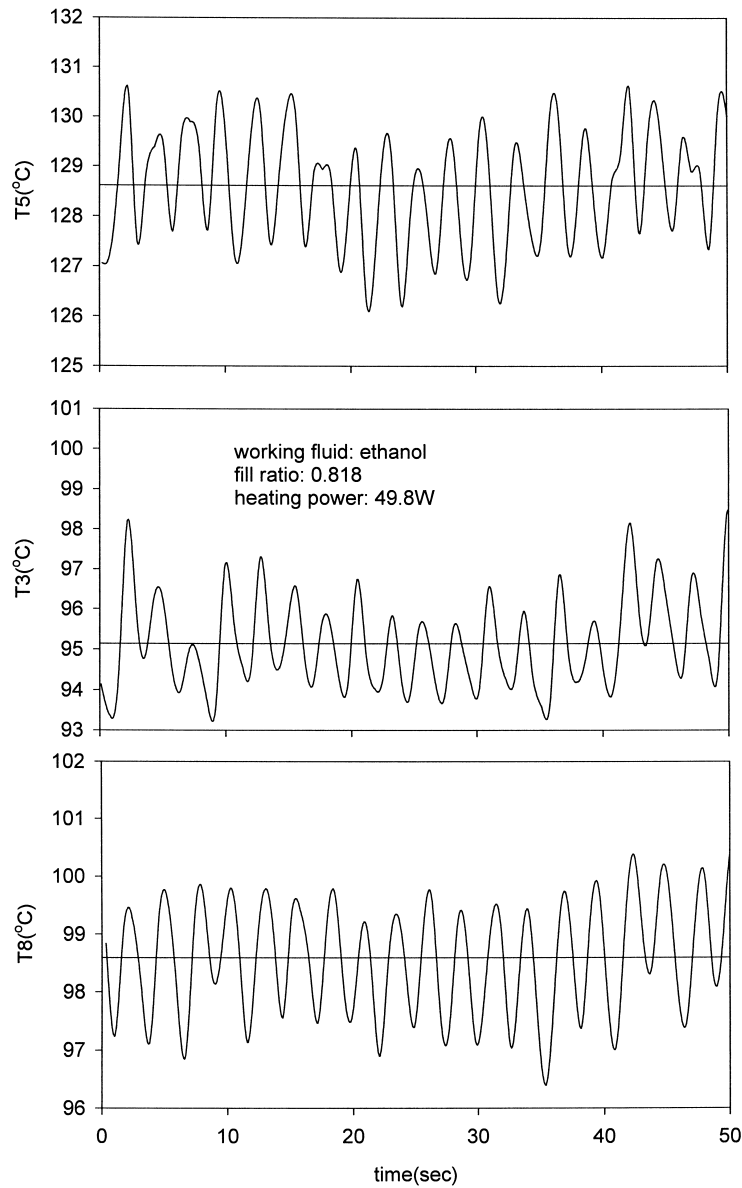


**Figure 5.** Thermal oscillation of the wall surface for ethanol.

understand that the minimum and maximum temperature differences are up to  $7^{\circ}\text{C}$  for some cycles.

Comparing Figures 4, 5, and 6, we understand that the cycle period of FC-72 is much smaller than those of ethanol and water, indicating that the oscillation process is much faster for FC-72 than for ethanol and water. From Table 2, we know that FC-72 possess a very low latent heat of evaporation. For the same heat received from the heating section, much more vapor mass can be produced for FC-72, resulting in enhanced

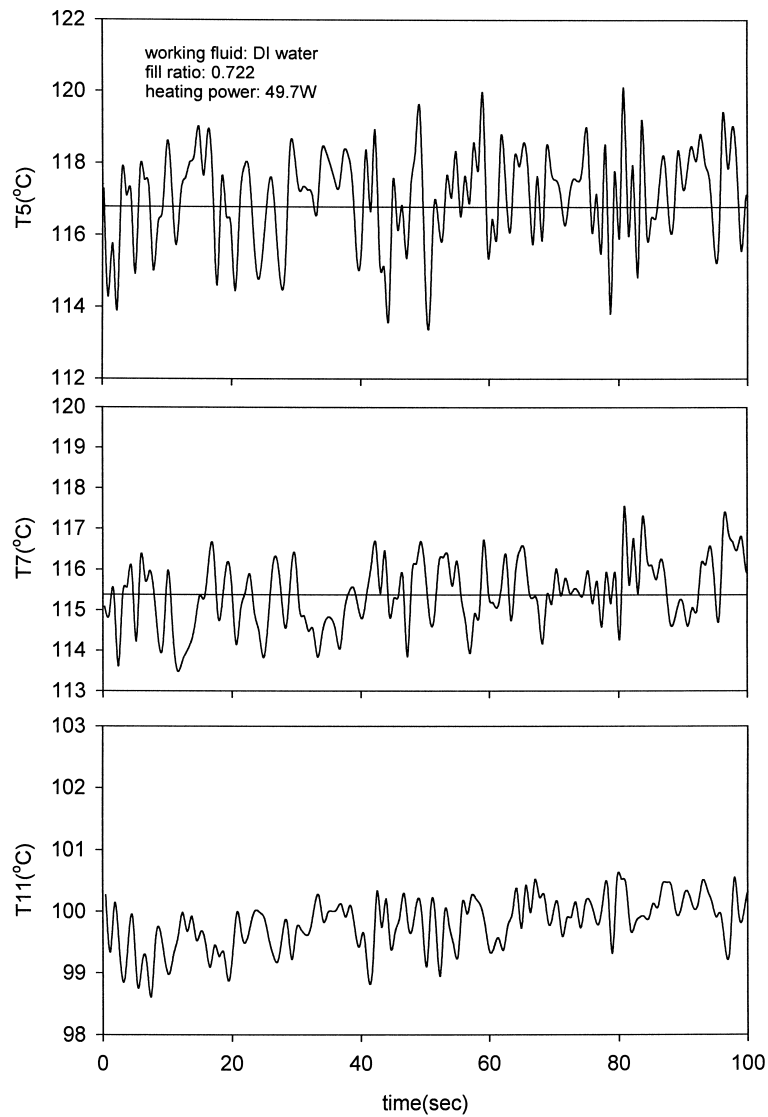


**Figure 6.** Thermal oscillation of the wall surface for water.

oscillation movement and thus shorter cycle period. If we perform power spectrum density (PSD) analysis on the random thermal oscillation wave for Figure 6, the characteristic cycle period for water is still longer than that for ethanol (Figure 5). Indeed, some short-cycle-period oscillations were identified as being imposed on the long-cycle-period oscillations for water. Such short-cycle-period oscillations are caused by the nonuniformly distributed vapor plug/liquid slugs inside the PHP.

The lower thermal oscillation amplitude of FC-72 is partially due to its lower surface tension compared to ethanol and water (see Table 2). The lower surface tension of FC-72 causes smaller pressure difference across the vapor/liquid interface [see Eq. (2)],

thus smaller temperature difference across the vapor/liquid interface. The present thermal oscillation analysis is consistent with the direct thermal oscillation measurements qualitatively. It should be noted that Shafii et al. [7, 8] proposed the numerical simulation of the PHP, and concluded that the major heat transfer is due to the sensible heat transfer, not the phase-change heat transfer. In terms of this hypothesis, there should be no thermal oscillation on the adiabatic section because there is no heat transfer between the wall surface and the fluid, which is in conflict with the present direct thermal oscillation measurements on the adiabatic section. The sensible heat transfer mechanism should be further confirmed by experiment.

### Unlooped PHP and Looped PHP

Figure 7 illustrates the comparisons of looped and unlooped PHPs for the same working fluid of FC-72, fill ratio of 70%, and heating power of 10 W. Also shown in Figure 7 is the looped PHP without any fluid inside the capillary tube for the same heating power. For the unlooped PHP and the looped PHP without liquid inside, similar axial temperature profiles are found, the mean temperatures in the heating section are very high, and the temperatures in the heat sink section are quite low, indicating the unlooped PHP does not work. In other words, heat accumulated in the heating section results in the high temperature distribution in the heating section. Under such conditions, heat received

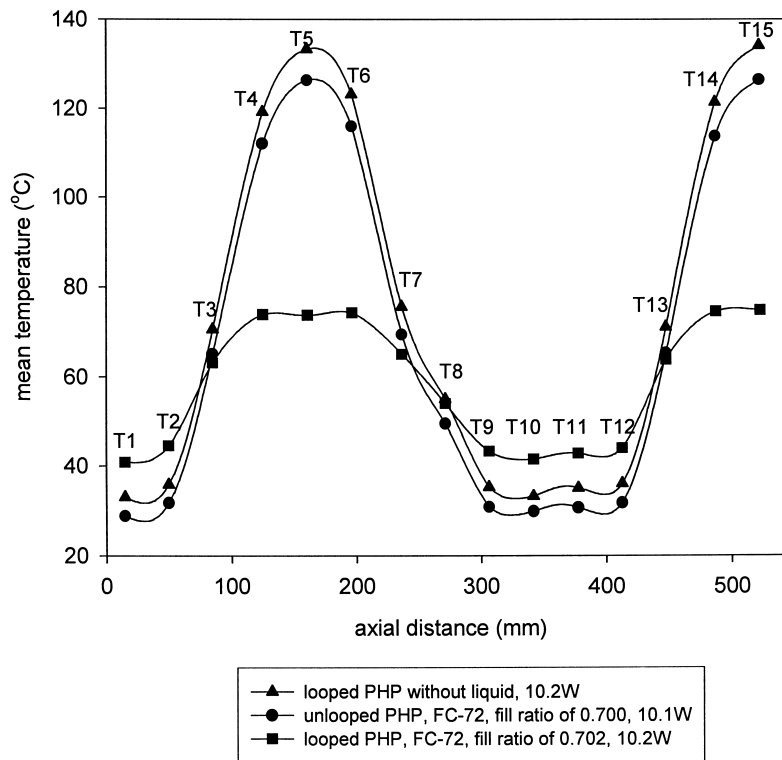


Figure 7. Comparisons of temperature profiles between unlooped and looped PHP.

from the heating wires is transferred to the heat sink only by axial heat conduction and to the environment due to the heat loss. We did not observe any temperature oscillation for the unlooped PHP. The unlooped PHP is not helpful for the fluid circulation inside the capillary tube and fully terminates the vapor plug/liquid slug movement inside the PHP, even though the temperatures in the heating section are quite high. Other run cases with different fill ratios and heating powers for the unlooped PHP were also tried, but the unlooped PHP never works. In the previous literatures, there are two types of PHPs, looped and unlooped ones. The present study gives direct evidence that the unlooped PHP does not work, at least for the present PHP configuration. Once the heating power is applied in the heating section of the looped PHP, the thermal oscillations occur and the PHP works well; the temperatures in the heating sections are quite low compared with those of the unlooped one (see Figure 7). The unlooped PHP data are provided only in Figure 7; others are all for the looped one.

### The Minimum Heating Power Activating the Working Looped PHP

For the looped PHP, we start to apply the heating power from a small value, such as 5 W, and stay under this run case for a long time, to observe the possible thermal oscillation. If there is no thermal oscillation observed, we increase the heating power with a small increment, such as 2 W, and stay at each heating power increment for a long time, to capture the minimum heating power activating the working PHP.

Surprisingly, we did find that there is a minimum heating power that activates the PHP. This minimum heating power is strongly dependent on the working fluids. Figure 8 shows the axial mean temperature profiles for the looped PHP with water as working

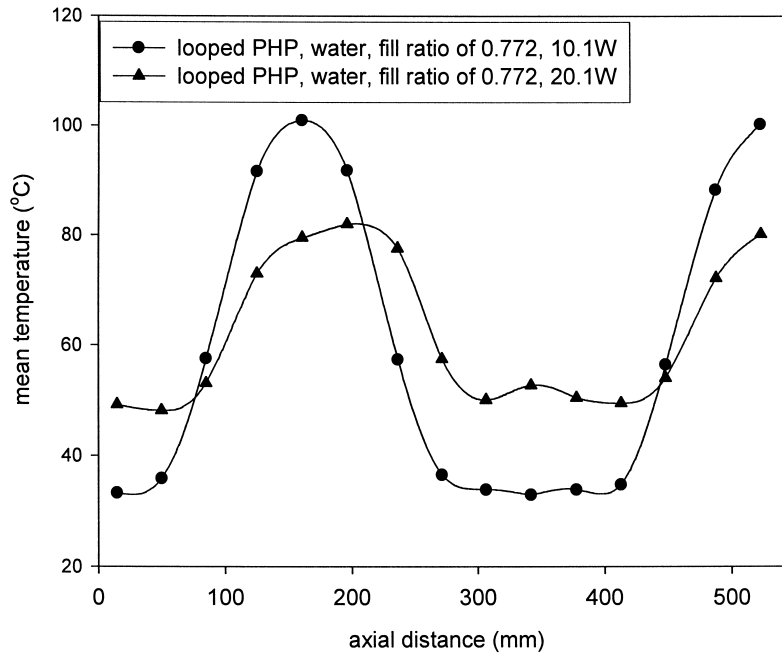


Figure 8. Minimum heating power activating the PHP working.

fluid, fill ratio of 0.772, and two different heating powers of 10.1 and 20.1 W. The mean temperatures in the heating section for the heating power of 10.1 W are much higher than those for 20.1 W, indicating that the present PHP at the heating power of 10 W is not working. Actually, the present PHP with water has a minimum heating power of 18 W. The heating power of 10.1 W (not working) is below the minimum heating power, while 20.1 W (working) is larger than the minimum heating power.

However, the minimum heating powers for ethanol and FC-72 are 10 and 8 W when the fill ratios are changed from 60% to 80%, respectively. The above minimum heating powers correspond to inner heat fluxes of 14.54, 8.08, and 6.46 kW/m<sup>2</sup> for water, ethanol, and FC-72, respectively.

It is noted that the minimum heating power is much smaller for FC-72 than for water. Also from Table 2, we know that the latent heat of evaporation is much smaller for FC-72 than for ethanol and water, indicating that the same heat can lead to much more vapor mass produced by the boiling process for FC-72. The large quantity of vapor mass produced in the heating section by FC-72 leads to larger vapor expansion in the heating section, resulting in the oscillation movement being easily activated. For a practical application point of view, we suggest that FC-72 be used for the low heating power condition.

### The Optimum Fill Ratio

It is well known that for the traditional micro/mini-heat pipe using triangular or rectangular microchannels, with or without wick structures, the fill ratio are in the range of 20–30%. Larger quantity of liquid filled inside the channels leads to liquid blockage of the channels and terminates the heat mass transfer process between the heating and the condensation sections. The boiling and condensation processes taking place inside traditional micro-heat pipes are stationary ones. However, in the PHP the oscillation movement of the vapor plug/liquid slugs and the smaller quantity of liquid inside the capillary tube results in large vapor volume in the channels, leading to even up the pressure difference between the heating and the condensation sections so the oscillation movement can be terminated. Therefore the PHP needs a higher fill ratio than traditional micro-heat pipes.

In the present study, the fill ratios vary from 60% to 80%. Higher fill ratios such as 90% were also tried, but the PHP does not work under such higher fill ratios for some run cases.

Figure 9 illustrates the mean axial temperature profiles for FC-72 at the fill ratios of 0.593, 0.702, 0.726, 0.774, and 0.820. Generally these temperature profiles are symmetric from T1 to T9 at the centerline of T5, and symmetric from T5 to T15 at the centerline of T10. T10 is a little higher than the neighboring temperatures of T9 and T11, because T10 is exposed directly in the air environment, while T9 and T11 are located in the heat sink sections. These curves are plotted at the given heating powers of 20, 30, and 40 W with an uncertainty of 0.2 W for different fill ratios. It is found that for all the heating powers, the mean temperatures in the heating section are lowest at the fill ratio of 0.726 (curves denoted by ■). Higher fill ratios of 0.774 and 0.820, denoted by ▼ and ◆, lead to higher temperatures in the heating sections.

Similar temperatures are provided for ethanol at the fill ratios of 0.600, 0.704, 0.756, and 0.818 in Figure 10. The heating powers are 20, 40, and 60 W with an uncertainty of

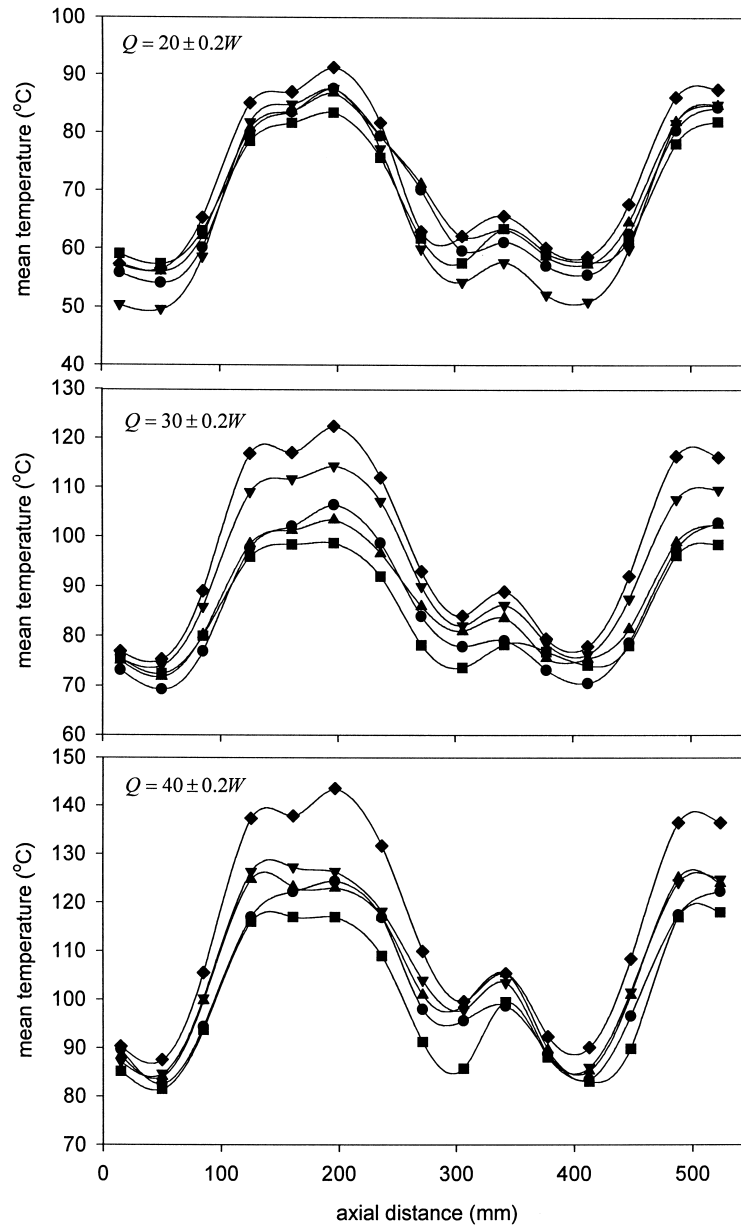


**Figure 9.** Effect of fill ratio on the PHP for FC-72 (●, fill ratio of 0.593; ▲, fill ratio of 0.702; ■, fill ratio of 0.726; ▼, fill ratio of 0.774; ◆, fill ratio of 0.820).



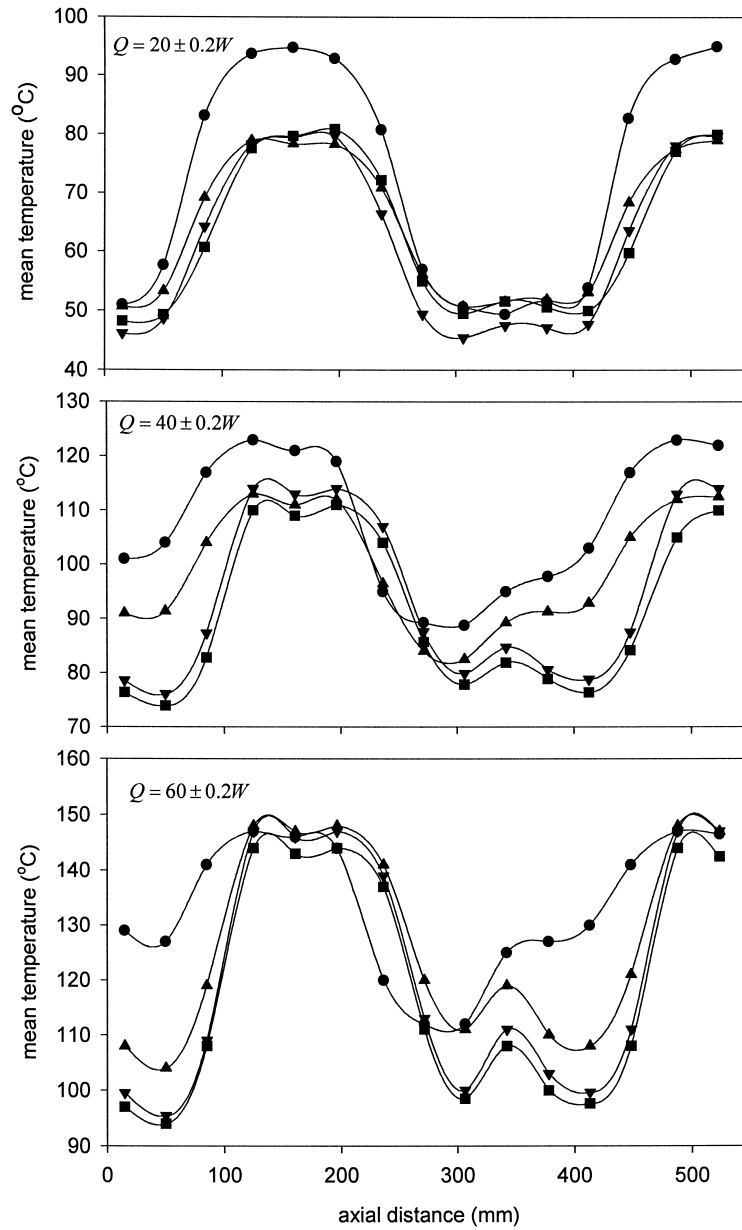


**Figure 10.** Effect of fill ratio on the PHP for ethanol (●, fill ratio of 0.600; ▲, fill ratio of 0.704; ■, fill ratio of 0.756; ▼, fill ratio of 0.818).

0.2 W. The mean temperatures in the heating sections for the fill ratios of 0.704, 0.756, and 0.818 show not much difference. However, the mean temperatures in the heating section are much higher for the smaller fill ratio of 0.600, especially at the heating powers of 20 and 40 W.

The mean temperature profiles for water at the fill ratios of 0.607, 0.722, 0.772, and 0.825 are plotted in Figure 11. The important finding is that the temperatures in the heating section are lower at the fill ratio of 0.722 (curves denoted by ▲) than at other fill ratios. Lower fill ratio of 0.607, and higher fill ratios of 0.772 and 0.825, result in higher temperatures in the heating section.

From the above observations, the optimal fill ratio for the three working fluids is around 70%. Lower fill ratios such as 60% and higher fill ratios such as 80% result in worse thermal performance of the looped PHP.

### Thermal Performance of the Present PHP for the Three Working Fluids

For a traditional heat pipe, one usually uses the temperature difference between the boiling and the condensation sections, and the thermal resistance to describe the thermal performance. Similarly, these terms are used here to describe the overall thermal performance of the looped PHP. The hot-side temperature is the averaged temperatures of T4, T5, T6, T14, and T15. The cold-side temperature is the averaged one including T1, T2, T8, T9, T11, and T12 (see Figure 1). They are written as

$$\begin{aligned} T_{\text{hot}} &= \frac{T4 + T5 + T6 + T14 + T15}{5} \\ T_{\text{cold}} &= \frac{T1 + T2 + T8 + T9 + T11 + T12}{6} \end{aligned} \quad (8)$$

The thermal resistance is defined as the temperature difference between the hot side and cold side divided by the total heating power.

Figure 12 illustrates the temperature differences and the thermal resistances of the looped PHP for the three working fluids at the fill ratio around 70%, which is recommended as the optimal value in the above section. The PHP with water as the working fluid has the lowest values of not only the temperature differences, but also the thermal resistances, among the three working fluids. The temperature difference curves have a minimum point for the three working fluids. Such minimum points occur at the heating power of 20 W for FC-72, 30 W for ethanol, and 40 W for water. Further increasing the heating power beyond the minimum points increases the temperature differences, especially for water. The thermal resistances have a sharp decrease with increasing heating power, then transfer to a very slight decrease and keep nearly constant at about 0.7°C/W for FC-72. The thermal resistances show similar trends, but oscillate around 0.7°C/W at heating power greater than 30 W for ethanol. The thermal resistances have a lowest value of 0.348°C/W at the heating power of 50 W for water. Further increasing the heating power leads to a sharp increase of the thermal resistances, thus deteriorating the heat transfer process. In general, the looped PHP with water as the working fluid provides the best thermal performance among the three working fluids, provided the heating power is larger than its minimum heating power as mentioned before.

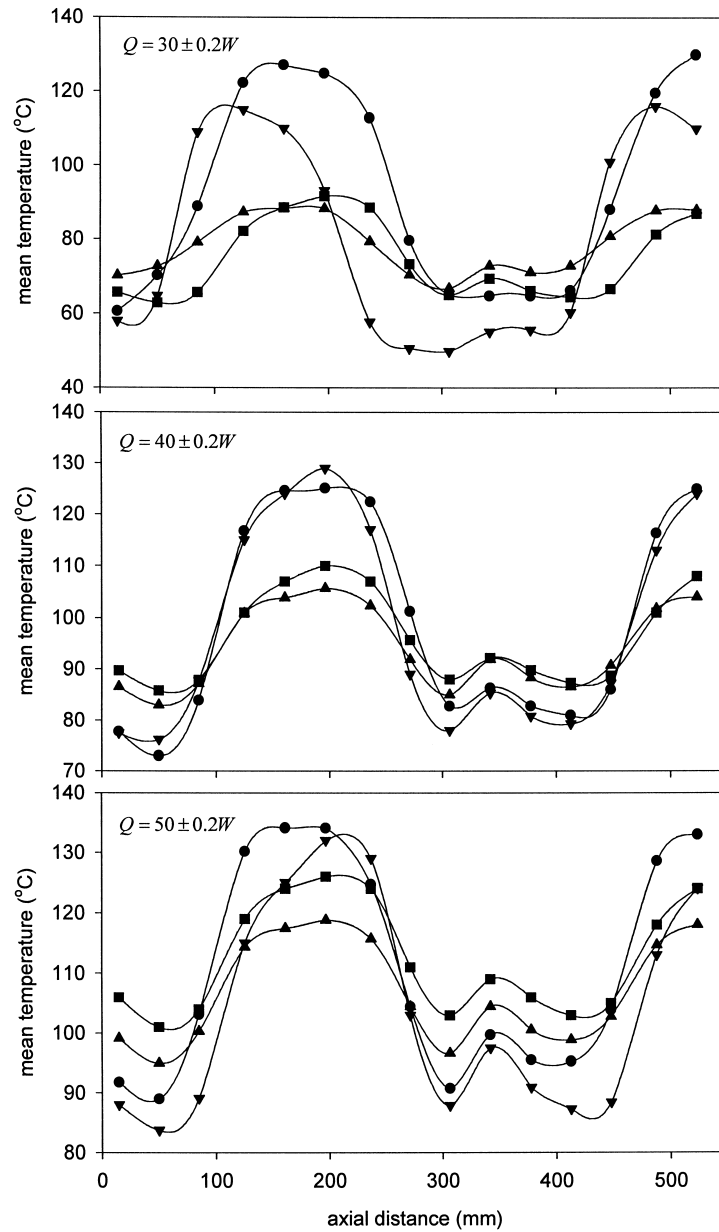


**Figure 11.** Effect of fill ratio on the PHP for water (●, fill ratio of 0.607; ▲, fill ratio of 0.722; ■, fill ratio of 0.772; ▼, fill ratio of 0.825).

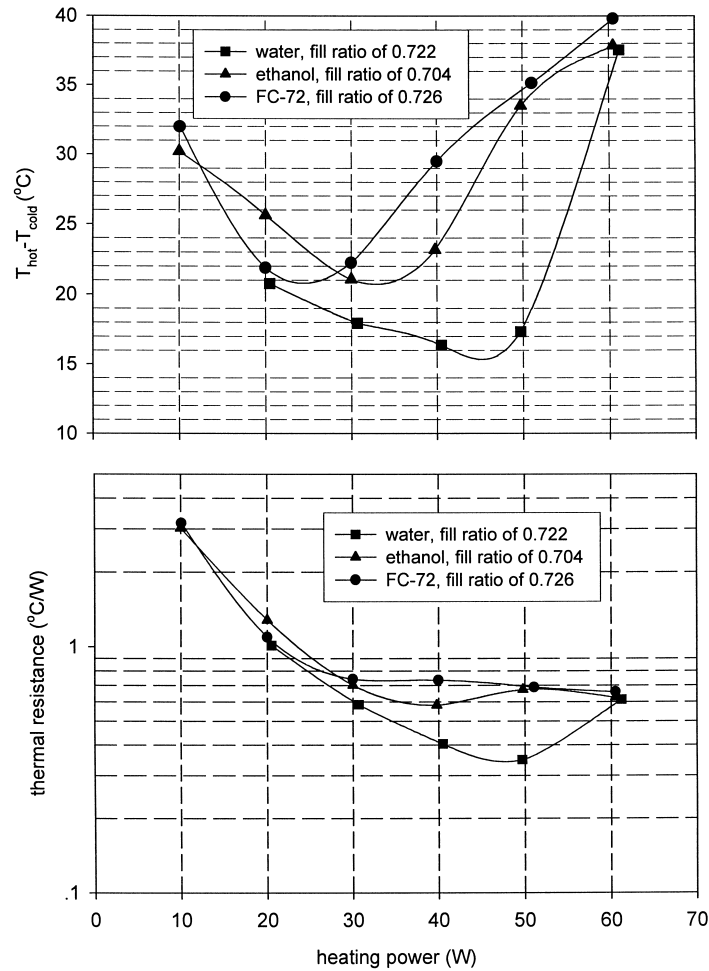


Figure 12. Overall thermal performance of the PHP for the three working fluids.

There is little experimental work performed on the thermal performance of the PHP in the open literature. However, the recent literature survey by Khandekar [10] indicated that the looped PHP with outer and inner diameters of 1.0 mm and 0.7 mm has average thermal resistances ranging from 0.64 to 1.16°C/W for the heating power range of 5–90 W, which can be comparable with the present thermal resistance measurements. Because the thermal resistances depend on many factors, i.e., the PHP configuration, the heating mode, the working fluids, etc., it is difficult to make direct comparisons.

## CONCLUSIONS

The detailed thermal oscillations of the wall surface of the PHP were measured for the three working fluids of FC-72, ethanol, and water. The conclusions are summarized as follows.

1. Periodic thermal oscillations are always detected with the three working fluids. It is found that the PHP with FC-72 has smaller oscillation amplitude, indicating smaller nonequilibrium temperature difference across the vapor/liquid interface, possibly due to the very small surface tension. The oscillation cycle period is much shorter for FC-72, indicating that the dynamic oscillation inside the capillary tube is much faster for FC-72 than for the other two fluids. The other two fluids, especially water, have a larger oscillation amplitude and much longer cycle period, compared with FC-72.
2. The unlooped PHP does not work, especially for the present PHP configuration. We strongly suggest that the unlooped PHP not be used for practical designs.
3. The looped PHPs with FC-72 and ethanol have a smaller minimum heating power that activates the PHP working than that with water. We suggest that FC-72 be used for the PHP at the lower heating rate. This is the major benefit of using FC-72 as the working fluid.
4. The experimentally determined optimal fill ratio is suggested to be 70% for the three working fluids. Lower fill ratios such as 60% and higher fill ratios such as 80% result in worse thermal performance of the looped PHP for all three working fluids.
5. The looped PHP with water as working fluid provides the best overall thermal performance. There are minimum points for the temperature differences, or the thermal resistances for the three fluids. Higher heating power beyond the minimum points deteriorates the heat transfer process.
6. The possible reasons inducing the above phenomena have been analyzed.

## REFERENCES

1. H. Akachi, Structure of a Heat Pipe, U.S. Patent 4921041, 1990.
2. W. H. Lee, H. S. Jung, J. H. Kim, and J. S. Kim, Flow Visualization of Oscillating Capillary Tube Heat Pipe, *Proc. 11th Int. Heat Pipe Conf.*, Tokyo, Japan, 1999, pp. 131–136.
3. Y. Miyazaki and M. Arikawa, Oscillatory Flow in the Oscillating Heat Pipe, *Proc. 11th Int. Heat Pipe Conf.*, Tokyo, Japan, 1999, pp. 143–148.
4. M. Schneider, S. Khandekar, P. Shafer, R. Kulenovic, and M. Groll, Visualization of Thermo-Fluid Dynamic Phenomena in Flat Plate Closed Looped Pulsating Heat Pipe, *6th Int. Heat Pipe Symp.*, Chiang Mai, Thailand, 2000, pp. 320–328.
5. T. N. Wong, B. Y. Tong, S. M. Lim, and K. T. Ooi, Theoretical Modeling of Pulsating Heat Pipe, *Proc. 11th Int. Heat Pipe Conf.*, Tokyo, Japan, 1999, pp. 159–163.
6. R. T. Dobson and T. M. Harms, Lumped Parameter Analysis of Closed and Open Oscillatory Heat Pipes, *Proc. 11th Int. Heat Pipe Conf.*, Tokyo, Japan, 1999, pp. 137–142.
7. M. B. Shafii, A. Faghri, and Y. W. Zhang, Thermal Modeling of Unlooped and Looped Pulsating Heat Pipes, *ASME J. Heat Transfer*, vol. 123, pp. 1159–1172, 2001.
8. M. B. Shafii, A. Faghri, and Y. W. Zhang, Analysis of Heat Transfer in Unlooped and Looped Pulsating Heat Pipes, *Int. J. Numer. Meth. Heat Fluid Flow*, vol. 12, no. 5, pp. 585–609, 2002.
9. Z. J. Zuo, M. T. North, and L. Ray, Combined Pulsating and Capillary Heat Pipe Mechanism for Cooling of High Heat Flux Electronics, Thermacore, Inc., [www.thermacore.com](http://www.thermacore.com).
10. S. Khandekar, M. Schneider, and M. Groll, Mathematical Modeling of Pulsating Heat Pipes: State of the Art and Future Challenges, *6th Int. Heat Pipe Symp.*, Chiang Mai, Thailand, 2000, pp. 123–130.